Radiostereometric analysis: comparison of radiation dose and precision in digital and computed radiography

Jorgensen, P.B.; Krag-Nielsen, N.; Lindgren, L.; Morup, R.M.S.; Kaptein, B.; Stilling, M.

Archives of Orthopaedic and Trauma Surgery (2023) 143:5919–5926
https://doi.org/10.1007/s00402-022-04674-0

HIP ARTHROPLASTY

Radiostereometric analysis: comparison of radiation dose and precision in digital and computed radiography

Peter Bo Jørgensen[1] · Nicolai Krag-Nielsen[2] · Lars Lindgren[2] · Rikke Margrethe Staghøj Mørup[1] · Bart Kaptein[3] · Maiken Stilling[1]

Received: 23 August 2022 / Accepted: 23 October 2022 / Published online: 23 November 2022

Abstract

Background Radiostereometric Analysis (RSA) is used to measure fixation of joint prosthesis. This study compared radiation dose and image quality of a digital radiography (DR) RSA system and a computed radiography (CR) RSA system in a clinical setting.

Methods RSA recordings of 24 hips and shoulders were analyzed. We compared two systems: (1) Arcoma T0 with ST-VI image plates and Profect CR-IR 363 reader to (2) AdoraRSA with CXDI-70C wireless DR detectors in a clinical uniplanar RSA set-up with a ± 20 degrees tube angulation and 35 cm × 43 cm detectors. Effective dose was calculated using dedicated software. Image quality was evaluated using calibration errors as calculated by the RSA software.

Results The mean dose for hips was 0.14 (SD 0.04) mSv in the CR system and 0.05 (SD 0.02) mSv in the DR system. The mean dose for shoulders was 0.16 (SD 0.07) mSv in the CR system and 0.09 (SD 0.03) mSv in the DR system. Radiation dose was 64% ($p < 0.001$) and 43% ($p = 0.03$) lower in the DR system compared with the CR system for hip and shoulder RSA, respectively. Image quality was better for the DR system with 60–80% less calibration errors compared to the CR system.

Conclusion Owing to highly efficient detectors and added filtration at the x-ray tubes, the DR system considerably reduced radiation dose compared with the CR system without compromising image quality.
Based on the findings in this study, we recommend replacing CR RSA systems with DR RSA systems.

Registration Patients were selected from clinical studies performed on the two systems and approved by the local ethics committee [20060165, M-20100112, M-20070082, M-20110224, and 20070258] and registered with ClinicalTrials.gov [NCT00408096, NCT01289834, NCT00913679, NCT02311179, and NCT00679120].

Keywords Radiostereometric analysis · Image quality · Radiation dose · Digital imaging · Implant migration

Introduction

Radiostereometric analysis (RSA) of a prosthesis over time provides a migration pattern, and clinical studies show that continuous migration is related to early mechanical failure. Prosthesis migration is measured with respect to small tantalum markers inserted in the periprosthetic bone and has sub-millimeter accuracy [1–4].

The RSA setup consists of two X-ray systems to create a stereo view. A calibration box with markers is used to calibrate the images and calculate the positions of the roentgen foci [2].

Over the last two decades, imaging techniques have improved from film/screen combinations to digital X-ray imaging based on computed radiography (CR) and digital radiography (DR) [5]. DR technology benefits clinical workflow considerably and may also reduce the radiation dose although influenced by factors like detective quantum efficiency, image processing methods, efficiency of the X-ray tube/filter combination, patient size and radiographic positioning [6].

✉ Peter Bo Jørgensen
pbjr@clin.au.dk

[1] AutoRSA Research Group, Orthopaedic Research Unit, Aarhus University Hospital, Palle Juul-Jensens, Boulevard 99, 8200 Aarhus N, Denmark

[2] Department of Radiology, Aarhus University Hospital, Aarhus, Denmark

[3] Biomechanics and Imaging Group (BIG), Leiden University Medical Center, Leiden, The Netherlands

RSA studies normally include 5 to 6 RSA recordings and radiosensitive tissue is radiated in hips (mainly bladder, ovaries/testicles, prostate and intestine tissue) and shoulder (mainly lung tissue). Still, little is known about the actual radiation dose. To our knowledge, only Teeuwisse et al. have reported the radiation dose of RSA imaging of different joints with conventional roentgen systems using film cassettes [7]. More recently, a phantom study was done to estimate radiation dose in hips for a modern DR RSA system [8]. Currently, the literature does not document benefits in radiation dose and image quality when changing from CR to DR RSA imaging in a clinical setting.

This study investigated the radiation dose and image quality in RSA procedures of the hip and shoulder comparing CR imaging technology with state-of-the art DR imaging technology Table 1.

Patients and methods

Patients

The study involved retrospective data on 12 patients (6 hips and 6 shoulders) examined using CR, and 12 patients (6 hips and 6 shoulders) examined using DR. Hip patients were mean 67.9 years (range 45–88) and shoulder patients were mean 63.1 years (range 44–73). The patients were matched concerning gender and BMI category according to WHO: Normal weight: 18.5–25, overweight 25–30, and obese > 30. These clinical factors have the highest effect on dose regulation. Mean BMI for CR recordings were 28.8 (SD 4.3) and 27.9 (SD 5.9) kg/m2 for hip and shoulder patients, respectively. Mean BMI for DR recordings were 26.4 (SD 3.4) and 28.5 (SD 3.9) kg/m2 for hip and shoulder patients, respectively (Table 2). No underweight patients (BMI < 18.5) were identified.

RSA recording systems

System 1 (CR) was the original RSA system in the facility: Arcoma T0 (Santax, Aarhus, Denmark) with ST-VI image plates and a Profect CR-IR 363 reader (Fujifilm, Tokyo, Japan). System 2 (DR), replacing the CR system, was AdoraRSA (Nordic Roentgen Technique, Hasselager, Denmark) with CXDI-70C wireless detectors (Canon, Tokyo, Japan) (Table 1).

RSA recording set-up and protocol

The stereoradiographic set-up for the two systems was similar with ceiling fixed roentgen sources and a 40-degree tube angulation. The CR and DR set-ups used the same carbon-fibre uni-planar calibration box (97 × 47 × 24 cm) with unfocussed scatter grids (35 × 43 cm), ratio 13:1, frequency 60 lines/cm carriage for all exposures (Carbonbox 24, Leiden University Medical Center, The

Table 1 System specifications of the CR and DR systems

	CR (System 1)	DR (System 2)
System name	Arcoma T0/Fuji	AdoraRSA/Canon CXDI-70C
Generator	Medira 65 kW	Indico IQ 80 kW
Radiation source	ArcoCeil T0	Varian A196/B130
CR reader	Fuji Profect CR- IR 363	-
Screens / detectors	ST-VI	Canon CXDI-70C, Wireless
Screen/detector size (cm)	35 × 43 cm	35 × 43 cm
Screen/detector size (pixels)	4280 × 3520 pixel	3408 × 2655
Resolution	5 lp/mm	4 lp/mm
Pixel size	100 µm	125 µm
Samples per pixel	3	1
Grey scale	10 bits	12 bits
Detective quantum efficiency	24% (5 µGy, 0 lp/mm)	60% (4 µGy, 0 lp/mm)
Fill factor	–	87%
View time	~60 s	~5 s
Material	Phosphor Granular (BaFBr Eu2 +)	Caesium iodide (CsI:TI)
Image capture		Large Area New-MIS sensor and TFT
Image processing software	Fuji 'Image Intelligence'	CXDI NERF

Lp line pair
CR Computed radiography
DR Digital radiography

Table 2 Body mass index (kg/m2) and age per group

	n	BMI (SD)	BMI range	Male	Female	Age (sd)	Age (range)
CR hip	6	28.8 (4.3)	24–34	3	3	71(14)	45–88
DR hip	6	26.4 (3.4)	23–31	3	3	64,2(8)	57–79
CR shoulder	6	27.9 (5.9)	21–36	3	3	64,2(6)	55–69
DR shoulder	6	28.5 (3.9)	23–33	4	2	62,2(10)	44–73

CR computed radiography

DR digital radiography

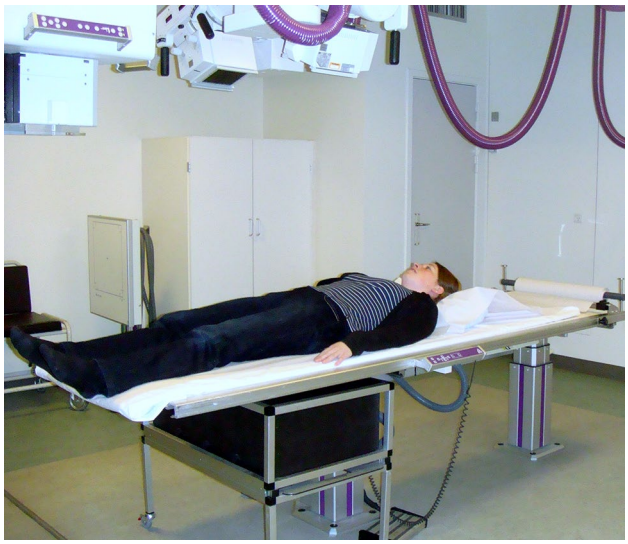

Fig. 1 The CR-system set-up for hip RSA with the patient in supine position. The calibration box is positioned transverse to the examination table

Fig. 2 The DR-system set-up for shoulder RSA with the patient in supine position and arms resting with the palm of the hand against the bed. The calibration box is positioned lengthwise to the examination table

Netherlands). This box has 25 1-mm fiducial markers in the lower plane and 16 1-mm control markers in the upper plane for each X-ray detector. Lateral/medial or cranio/caudal projections for hip and shoulder stereoradiographs were made respectively. Detectors were placed parallel to the ceiling resulting in a 20-degree entry angle of the central X-ray beams. The imaging detectors were placed opposite to the related X-ray tube, X-ray beams were crossed in a 40-degree angle in the anatomy of interest (Figs. 1 and 2).

Both systems were operated by a team of three radiographers experienced in RSA. The protocol was similar for both systems (RSA set-up and patient position), but exposure settings (kV and mAs) were optimized for each patient in both systems. The stereo radiographs were assessed for visibility of calibration markers, bone markers and implants by the radiographer. We used the lowest dose to provide sufficient image quality. The exposure settings are given in Table 3. The radiographer performed a subjective visual judgement of the quality of the stereoradiographs based on marker-visibility and bony anatomy. In most RSAs, the whole detector plate is imaged and collimation is thus done based on the detector (including all calibration box markers), not on the anatomy of interest.

Dose calculations

To calculate the effective dose, imaging parameters such as collimation and anatomical positioning were evaluated from clinical patient data retrieved from the Picture Archiving and Communication System (PACS). All exposures in both systems were done with manual exposure technique settings and large focus. We calculated the radiation dose for shoulder and hip RSA exposures.

On both systems, the projections, exposure, filtration and geometrical settings were constant for the recordings. The settings were optimized for clinical use. Hence,

Table 3 Exposure, filtration, kVp accuracy, mAs linearity and geometrical settings for all procedures in the study

X-ray tube and geometry settings	Hip projections				Shoulder projections			
	CR (System 1)		DR (System 2)		CR (System 1)		DR (System 2)	
	Tube 1	Tube 2	Tube 1	Tube 2	Tube 1	Tube 2	Tube 1	Tube 2
kVp	90–96	90–96	90–110	90–110	90–96	90–96	75–80	75–80
kVp accuracy (%)	< 2.1	< 1.9	< 0.6	< 1.0	< 2.1	< 1.9	< 0.6	< 1.0
mAs	13–20	13–20	5–8	6.3–10	10–25	10–25	5–6	5–6
mAs linearity (%)	< 3	< 3.8	< 4.0	< 9.7	< 3	< 3.8	< 4.0	< 9.7
Added filtration	2 mm Al	2 mm Al	1 mm Al + 0.1 mm Cu	1 mm Al + 0.1 mm Cu	2 mm Al	2 mm Al	None	None
FID cm	158		150		158		150	
FSD cm	105–115		98–104		111–122		105–115	
PED cm	28		28		28		28	

CR computed radiography, *DR* digital radiography, *FID* focus image distance, *FSD* focus skin distance, *PED* Phantom exit distance

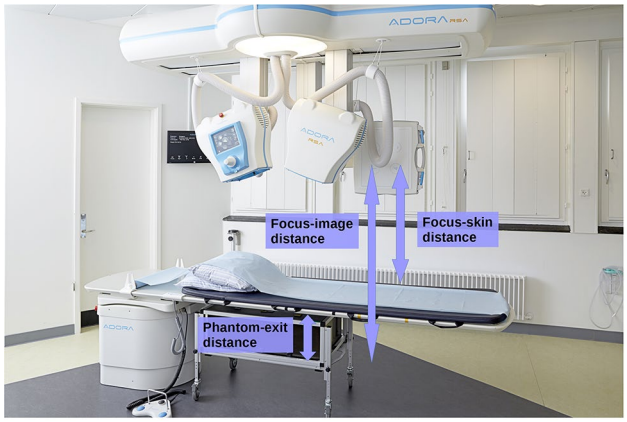

Fig. 3 The distances required to calculate the geometrical beam properties

a number of parameters were considered such as patient positioning, sufficient image quality for RSA analysis, and radiation dose reduction (Table 2) [9].

Dose calculation and image analysis software

When X-ray photons interact with matter, different processes may occur depending on photon energy and properties of the material. In this stochastic process, it is achievable to predict the possibility of an interaction process for a certain photon, depending on the photon energy and tissue types. The PCXMC 2.0 (STUK, Helsinki, Finland) is a computer program designed to calculate these probabilities and estimate them as medical X-ray doses. It uses the Monte Carlo simulation method, based on the mathematical hermaphrodite phantoms of Cristy and Eckerman and enables scaling to calculate doses for patients with different height and weight from these phantoms [10].

Focus-skin-distance (FSD) and incoming beam size were automatically derived in the software from the parameters; focus-image-distance (FID), phantom-exit-distance (PED), image field size, patient height, and weight (Fig. 3).

Furthermore, the software utilized information on patient size (height and weight), projection angle, X-ray tube potential (kV), X-ray tube anode angle, filtration and incoming dose quantity. The latter can be given as either incident air kerma (mGy), dose-area-product ($mGycm^2$), entrance-exposure (mR), exposure-area-product (Rcm^2) or current–time-product (mAs). The effective dose can be calculated in weighted factors ICRP60 and ICRP103. We used the PCXMC tool to calculate the individual effective patient doses for hips (2 radiographs/views for 6 recordings on 2 systems) and for shoulders (2 radiographs/views for 6 recordings on two systems).

Model-based RSA 4.10 (RSA*core*, LUMC, Leiden, The Netherlands) is a widely used analysis software to evaluate implant migration in radiostereometric images. First, the software detects the positions of calibration and bone markers automatically using an extension and improvement of the circle finding algorithm described by Duda et al. [11]. Then, the marker positions are enhanced to sub-pixel accuracy by estimating a paraboloid through the gray-scale profile of the projected markers [12].

Calibration of the RSA set-up is calculated based on the detected markers in the radiostereometric images and known marker positions for the calibration box. The fiducial markers at the bottom of the calibration box are used to calibrate the image plane, and the control markers at the top of the calibration box are used to calculate the focus positions (Fig. 4).

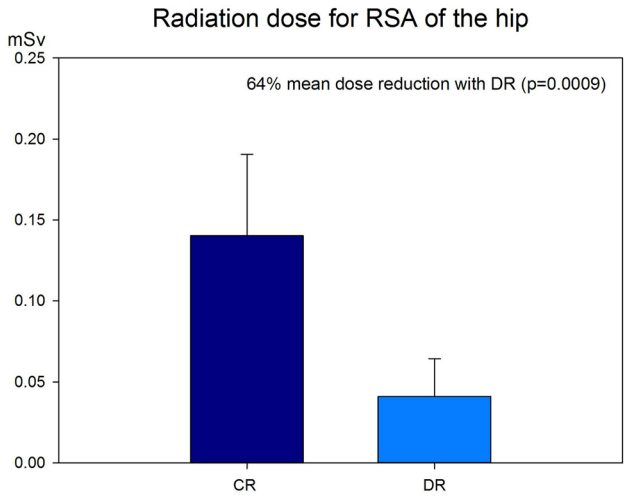

Fig. 4 Analysis of an RSA image of a total hip arthroplasty and a shoulder resurfacing implant. 12 control markers (top layer of the calibration box) in each image calibrate the roentgen foci. 25 fiducial markers (bottom layer of the calibration box) in each image calibrate the image plane. Bone markers make up a rigid body reference of the bone. The edge of the hip or shoulder implant is detected and projected to a CAD implant model

Image precision and quality

Objective image quality was defined by the ability of the RSA algorithms to reconstruct the 3D marker positions of the calibration box and roentgen focus positions, which is expressed as the calibration error. The calibration error consists of a fiducial error, defined as the root-mean-square (RMS) distance between the reconstructed and the known fiducial marker positions, and a control error, defined as the RMS distance between the projection lines of the control markers and the calculated focus position [1].

Different calibration boxes have different calibration errors depending on the box design i.e., the number of markers, the marker patterns, and the distance between marker planes. Based on our clinical experience, the optimal errors (all markers visible and used) that could be obtained in our set-up for the utilized Carbonbox 24 was 0.106 mm for control error and 0.016 mm for fiducial error. We used standard software settings without manually adding or editing marker projections for an objective evaluation of measured image quality with CR and DR. We compared calibration errors, and the automatic detection percentage of bone and calibration box markers with a manual count of visual calibration box markers as the reference [2, 3].

Subjective image quality was rated by the analysist for each recording as either poor, sufficient or excellent.

Validation of current–time-product

The most accurate way to determine dose quantity is to measure it directly in the beam (dose-area-product), instead of using current–time-product. Dose quantity from different X-ray tube/collimator combinations will vary, according to differences in X-ray tube design, filtration, collimator design and wear of components; the current–time-product does not compensate for this. Measuring the dose quantity directly in the beam was not possible in this study, because the equipment had already been changed before the start of the study, and the current–time-product was used. Due to this potential uncertainty, the dose output from two impartial X-ray tube/collimator combinations was measured under the same conditions used for RSA imaging with CR as a reference.

Statistics

Data for effective patient doses were normally distributed (Shapiro–Wilk test), and data variation was similar using CR and DR for both shoulders and hips (*f*-test). A two-sample Student's *t*-test with equal variation was used to test group (DR vs CR) and subgroup (BMI classification) differences was tested using Kruskal–Wallis. Statistical significance was set at $p < 0.05$.

Results

The kilovolt (kV) settings for hip projections ranged between 90 and 96 kV for CR and were fixed at 90 kV for DR, except for one obese patient recorded at 110 kV. The current–time-product was reduced from 13–20 for CR to 5–10 mAs for DR. In shoulder projections, exposure parameters were lowered even more; kV was reduced from 90–96 to 75–80, and mAs from 10–25 to 5–6. Thus, the mAs settings for DR were roughly halved compared to CR.

The patient dose was lowered from 0.14 (SD 0.04) mSv to 0.05 (SD 0.02) mSv on average for hip projections ($p < 0.001$). With no added filtration at the X-ray tube, the patient dose was lowered from 0.16 (SD 0.07) mSv to 0.09 (SD 0.03) mSv on average for shoulder projections ($p = 0.03$). The radiation dose within CR and DR systems was similar in BMI sub-groups for both hips ($p > 0.1$) and shoulders ($p > 0.2$). Overall, the DR system reduced patient dose by 64% for hip projections and by 43% for shoulder projections compared with the CR system (Fig. 5, Supplementary Table 1).

The image quality of DR was significantly better than CR, with 60—80% lower calibration errors for both hip

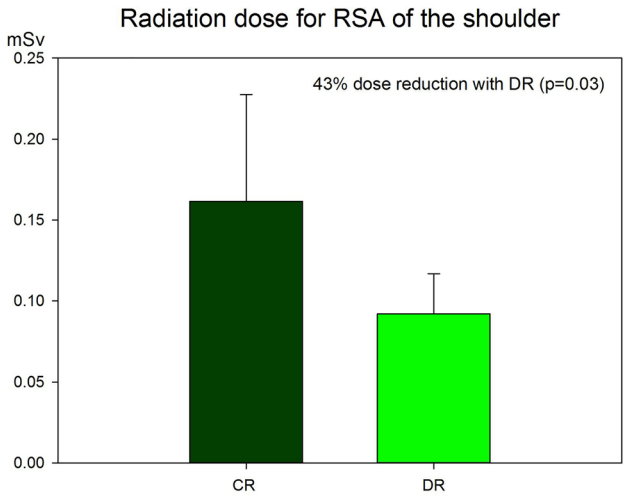

Fig. 5 Dose reduction with the DR system compared to the CR system for hip and shoulder projections. Mean values are given in the bars with standard deviation in the error bars

and shoulder RSA recordings (Table 3). Correspondingly, subjective image quality was rated better for the DR images (Table 4).

The validation of the current–time (mAs) product showed that the dose output from CR was 12.2% higher on average than in the two impartial tubes. This potential uncertainty must be taken into account when interpreting the results Table 5.

Discussion

The key findings in this study were that changing the RSA system from CR to DR reduced the patient radiation dose in RSA examinations and improved image quality. With a state-of-the-art DR RSA, we showed radiation doses of 0.09 mSv per shoulder RSA image and 0.05 mSv per hip RSA image. The main reason for this improvement is probably the high Detector Quantum Efficiency in the Canon CXDI-70C detectors of DR.

Hip projections on the CR RSA system had an average effective dose of 0.144 mSv, which corresponds well with the effective dose of 0.150 mSv reported by Teeuwisse et al. on a film-based RSA system [7]. The mAs settings for DR were roughly halved compared to CR, and the patient dose was thus roughly halved due to this change alone. As a result, the radiation dose in this clinical study corresponded well with the findings of Blom et al. for BMI group 1 and 2, where BMI group 3 received a higher radiation dose due to more soft tissue [8]. Unfortunately, some of this reduction was cancelled for shoulder recordings due to no added filtration at shoulder projections. If filtration was used, a dose reduction could probably be obtained.

Filtration

In this study, added filtration of 2 mm Al was used as a standard for all applications on CR. For hip projections on DR, a change in filtration to 1 mm Al + 0.1 mm Cu still resulted in improved image quality in terms of significantly lower calibration errors. However, the auto-detection percentage of bone markers in the RSA software was slightly lower compared with images from CR. For shoulder projections, 2 mm Al filtration was used for CR, but the best image

Table 5 Subjective image quality rated by the analysist

	CR (System 1)	DR (System 2)
Poor	2	0
Sufficient	7	5
Excellent	3	7

CR Computed radiography
DR Digital radiography

Table 4 Image quality assessment expressed as software marker recognition and given as percentage of the total number, and calibration error assessment (combined for left and right images) using a commercially available radiostereometric analysis software [3]

	CR Shoulder ($n=6$)	DR Shoulder ($n=6$)	CR Hip ($n=6$)	DR Hip ($n=6$)
Fiducial markers *(% detection)*	94	91	86	85
Fiducial error *(95% CI)*	0.125 (0.117;0.133)	0.020 (0.017;0.024)	0.125 (0.111;0.138)	0.026 (0.022;0.030)
Control markers *(% detection)*	94	96	88	90
Control error *(95% CI)*	0.409 (0.374;0.444)	0.125 (0.094;0.156)	0.466 (0.418;0.513)	0.133 (0.091;0.185)
Bone markers humerus *(% detection)*	72	58		
Bone markers femur *(% detection)*			87	80
Bone markers acetabulum *(% detection)*			49	34

Fiducial error = Image deformation error after calibration, Control error = root mean square of the distances between the projection lines of the control markers and the calculated focus position

quality results for DR turned out to be with no added filtration at all, due to thinner anatomy in this area.

Imaging detectors

The Canon CXDI 70C has a spatial resolution of 4 lp/mm, while the Fuji CR system has a spatial resolution of 5 lp/mm. Unfortunately, the Fuji CR system has imaging artefacts such as geometric distortions caused by mechanical imperfections (roller artefacts) during the digitization of the detector plate [13]. The artefacts contribute to a higher level of fiducial and control errors for CR.

Another contribution to high precision and low dose of the DR detectors is the high DQE. Even though the RSA software detected slightly fewer bone markers from CR to DR, there was not a significant loss of information as shown in Table 3. This supports that the dose efficiency of the Canon CXDI-70C detectors is much higher than in the Fuji CR system. The fact that DR is often more responsive compared to CR is supported by the literature and in our case also by the DQE specifications of the systems [6].

Limitations

It would have been optimal to examine the same patients in both the DR and CR systems, but unfortunately such data were not available.

It would have been desirable to measure the incoming dose quantity from CR directly in the beam. However, the RSA system was changed from CR to DR before this retrospective study was initiated and incoming dose quantity data were not available.

In conclusion, the radiation dose in RSA is particularly important when investigating the anatomy of organs sensitive to radiation doses. Furthermore, RSA imaging often involves repetitive follow-up imaging, which results in accumulated exposure to radiation for patients. We showed that changing from a CR to a DR RSA system approximately halved the patient radiation dose for hip and shoulder RSA examinations and improved image quality. Thus, we recommend that research facilities consider replacing CR RSA systems with DR RSA systems to improve image quality and lower radiation dose for patients.

Supplementary Information The online version contains supplementary material available at https://doi.org/10.1007/s00402-022-04674-0.

Author contributions PBJ, NKN, BK and MS designed and wrote the manuscript, and RMSM performed the image analyses. All contributed to the data interpretation and critical revision of the manuscript.

Funding The study was performed under the Innovation Fund Denmark Grant 69–2013-1 "Transforming radiological technology for assessment of implant fixation: from research tool to clinical application". None of the authors report any conflicts of interest.

Availability of data and materials Due to GDPR and the sensitive nature of x-rays, sharing of raw data is not possible. However, we will try to accommodate any reasonable request for sharing anonymized data.

Declarations

Competing interests Financial interests: The authors declare they have no financial interests. Non-financial interests: Authors Bart Kaptein and Maiken Stilling are on the board of The International Radiostereometry Society.

Ethics approval and consent to participate Patients were selected from clinical studies performed on the two systems and approved by the local ethics committee [20060165, M-20100112, M-20070082, M-20110224, and 20070258] and registered with ClinicalTrials.gov [NCT00408096, NCT01289834, NCT00913679, NCT02311179, and NCT00679120].

Consent for publication Not applicable.

References

1. Selvik G (1989) Roentgen stereophotogrammetry. A method for the study of the kinematics of the skeletal system. Acta Orthop Scand Suppl 232:1–51. https://doi.org/10.3109/17453678909154184
2. Valstar ER, Nelissen RGHH, Reiber JHC, Rozing PM (2002) The use of Roentgen stereophotogrammetry to study micromotion of orthopaedic implants. ISPRS J Photogramm Remote Sens 56:376–389. https://doi.org/10.1016/s0924-2716(02)00064-3
3. Kaptein BL, Valstar ER, Stoel BC, Rozing PM, Reiber JHC (2003) A new model-based RSA method validated using CAD models and models from reversed engineering. J Biomech 36:873–882. https://doi.org/10.1016/s0021-9290(03)00002-2
4. Karrholm J, Gill RH, Valstar ER (2006) The history and future of radiostereometric analysis. Clin Orthop Relat Res 448:10–21. https://doi.org/10.1097/01.blo.0000224001.95141.fe
5. Korner M, Weber CH, Wirth S et al (2007) Advances in digital radiography: physical principles and system overview. Radiographics 27:675–686. https://doi.org/10.1148/rg.273065075
6. Neitzel U (2005) Status and prospects of digital detector technology for CR and DR. Radiat Prot Dosimetry 114:32–38. https://doi.org/10.1093/rpd/nch532
7. Teeuwisse W BR, Geleijns J (1998) Stralenbelasting bij orthopedische radiologie n.d. Gamma:3.
8. Blom IF, Koster LA, Brinke BT, Mathijssen NMC (2020) Effective radiation dose in radiostereometric analysis of the hip. Acta Orthop 91:390–395. https://doi.org/10.1080/17453674.2020.1767443
9. Lindgren LJP, Mørup RMS, Jensen M, Rømer L, Kaptein B, Stilling M (2019) Similar patient positioning: A key factor in follow-up studies when using model-based radiostereometric analysis of the hip. Radiography. https://doi.org/10.1016/j.radi.2019.10.009.10.1016/j.radi.2019.10.009
10. Tapiovaara M, Siiskonen T (2008) A PC-based Monte Carlo program for calculating patient doses in medical x-ray examinations.
11. Duda RO, Hart PE (1972) Use of the Hough transformation to detect lines and curves in pictures. Commun ACM 15:11–15. https://doi.org/10.1145/361237.361242
12. Vrooman HA, Valstar ER, Brand GJ et al (1998) Fast and accurate automated measurements in digitized stereophotogrammetric radiographs. J Biomech 31:491–498. https://doi.org/10.1016/s0021-9290(98)00025-6

13. Shetty CM, Barthur A, Kambadakone A, Narayanan N, Kv R (2011) Computed radiography image artifacts revisited. AJR Am J Roentgenol 196:W37-47. https://doi.org/10.2214/AJR.10.5563